Hindawi Publishing Corporation
EURASIP Journal on Image and Video Processing
Volume 2007, Article ID 37843, 11 pages
doi:10.1155/2007/37843

Research Article

Quadratic Interpolation and Linear Lifting Design

Joel Solé and Philippe Salembier

Department of Signal Theory and Communications, Technical University of Catalonia (UPC), Jordi Girona 1–3, Edifici D5, Campus Nord, Barcelona 08034, Spain

Received 11 August 2006; Revised 18 December 2006; Accepted 28 December 2006

Recommended by Béatrice Pesquet-Popescu

A quadratic image interpolation method is stated. The formulation is connected to the optimization of lifting steps. This relation triggers the exploration of several interpolation possibilities within the same context, which uses the theory of convex optimization to minimize quadratic functions with linear constraints. The methods consider possible knowledge available from a given application. A set of linear equality constraints that relate wavelet bases and coefficients with the underlying signal is introduced in the formulation. As a consequence, the formulation turns out to be adequate for the design of lifting steps. The resulting steps are related to the prediction minimizing the detail signal energy and to the update minimizing the l^2-norm of the approximation signal gradient. Results are reported for the interpolation methods in terms of PSNR and also, coding results are given for the new update lifting steps.

1. INTRODUCTION

The lifting scheme [1] is a method to create biorthogonal wavelet filters from other ones. Despite the amount of research effort dedicated to the design and optimization of lifting filters since the scheme was proposed, many works (p.e., [2–4]) that contribute ideas to improve existing lifting steps with new optimization criteria and algorithms keep appearing. Certainly, there is room for contributions, specially in space-varying, signal-dependant, and adaptive liftings. Even in the linear setting, there are lines that deserve a further study. This paper follows the works [5, 6]. It proposes a linear framework for the design of lifting steps based on adaptive quadratic interpolation methods. First, a family of interpolation methods is presented. The interpolation is employed for the design of prediction and update lifting steps. It is assumed that an improvement in the interpolation implies an improvement in the subsequent lifting steps.

The prediction step extracts the redundancy existing in the odd samples from the even samples, so interpolative functions are a reasonable choice as initial prediction lifting steps. An adaptive quadratic interpolation method is proposed in [7], which is outlined in Section 2. The interpolation signal is found by means of the optimal recovery theory. We have observed that the problem statement may be reformulated as the minimization of a quadratic function with linear equality constraints. This insight provides all the resources and flexibility coming from the convex optimization theory to solve the problem. Furthermore, the initial problem statement may be modified in many different ways and the convex optimization theory still offers solutions. These variations are presented in Section 3.

This flexibility also allows the design of lifting steps with different criteria than the usual vanishing moments and spectral considerations. First, linear constraints are changed. Transformed coefficients are the inner product of wavelet basis vectors with the signal data. These products are new linear constraints introduced in the formulation. This fact permits the construction of initial prediction steps as well as the subsequent prediction and update steps for which the spatial interpolation interpretation is not straightforward.

Sections 5 and 6 present the design of prediction and update steps, respectively. Experiments are explained in Section 7. Results for the different interpolation methods are given in a setting linked to the lifting scheme. Lifting steps performance is assessed by means of the bit rate of compressed images. Finally, main conclusions are drawn in Section 8.

Notation 1. Boldface uppercase letters denote matrices, boldface lowercase letters denote the column vectors, uppercase

italics denote sets, and lowercase italics denote scalars. Indexes are omitted for short when they are clear from the context.

2. QUADRATIC INTERPOLATION

An adaptive interpolation method based on the quadratic signal class determined from the local image behavior is presented in [7]. We reformulate the method and propose several variations on it that consider additional knowledge available from the application at hand.

The described methods are based on two steps. First, a set to which the signal belongs (or a signal model) is determined. Second, the interpolation that best fits the model given the local signal is found. The first step is common for all the methods, whereas the second one is modified according to the available information. This section presents the first part and derives an optimal solution. This initial solution is retaken in Sections 5 and 6 with the goal of designing lifting steps. Section 3 describes alternative formulations.

A quadratic signal class $\mathcal{K}$ is defined as $\mathcal{K} = \{\mathbf{x} \in \mathbb{R}^n : \mathbf{x}^T\mathbf{Q}\mathbf{x} \leq \epsilon\}$. The choice of a quadratic model is practical because it can be easily determined using training data. The quadratic signal class is established by means of m image patches $\mathcal{S} = \{\mathbf{x}_1, \ldots, \mathbf{x}_m\}$ representative of the local data. Patches may be extracted from an upsampling and filtering of the image or from other images. Patches are high density, that is, they have the same resolution as the interpolated image. Therefore, if patches are extracted from the image to be interpolated, then an initial interpolation method is required and the proposed methods aim at improving the initial result.

Figure 1 depicts an example of image to be interpolated (the black pixels), and the high-resolution image (which includes the light pixels). The training set has to be selected. One direct approach of selecting the elements in $\mathcal{S}$ is based on the proximity of their locations to the position of the vector being modeled. In this case, patches are generated from the local neighborhood. For example, in Figure 1 the center patch

$$\mathbf{x} = \begin{pmatrix} x_{(2,2)} & x_{(2,3)} & x_{(2,4)} & x_{(2,5)} & x_{(3,2)} & \cdots & x_{(5,5)} \end{pmatrix}^T \tag{1}$$

may be modeled by the quadratic signal class of the set

$$\mathcal{S} = \left\{ \begin{pmatrix} x_{(0,0)} \\ x_{(0,1)} \\ \vdots \\ x_{(3,3)} \end{pmatrix}, \ldots, \begin{pmatrix} x_{(4,4)} \\ x_{(4,5)} \\ \vdots \\ x_{(7,7)} \end{pmatrix} \right\}, \tag{2}$$

where $\mathcal{S}$ is formed by choosing all the possible 4×4 image blocks in the 8×8 region of the figure.

Matrix $\mathbf{S}$ is formed by arranging the image patches in $\mathcal{S}$ as columns: $\mathbf{S} = (\mathbf{x}_1 \cdots \mathbf{x}_m)$. The solution image patch $\mathbf{x}$ is imposed to be a linear combination of the training set $\mathcal{S}$ through a column vector $\mathbf{c}$:

$$\mathbf{S}\mathbf{c} = \mathbf{x}. \tag{3}$$

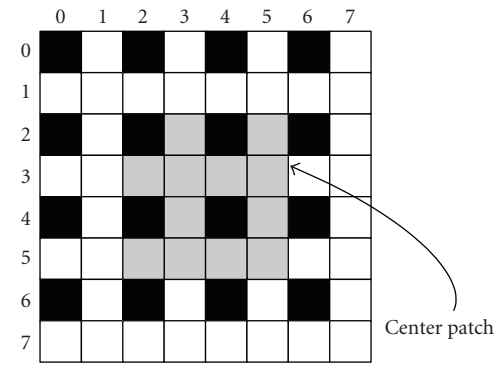

Figure 1: Local high density image used for selecting $\mathcal{S}$ to estimate the quadratic class for the center 4×4 patch (dark pixels are part of the decimated image).

As discussed in [7], vectors in $\mathbf{S}$ are similar among themselves and $\mathbf{x}$ is similar to the vectors in $\mathbf{S}$ when $\mathbf{c}$ has small energy,

$$\|\mathbf{c}\|^2 = \mathbf{c}^T\mathbf{c} = \mathbf{x}^T\left(\mathbf{S}\mathbf{S}^T\right)^{-1}, \quad \mathbf{x} \leq \epsilon. \tag{4}$$

In this sense, good interpolators $\mathbf{x}$ for the quadratic class determined by $(\mathbf{S}\mathbf{S}^T)^{-1}$ are expanded with the weighting vectors $\mathbf{c}$ of energy bounded by some ϵ.

Once the high density class $\mathcal{S}$ is determined, the optimal interpolated vector $\mathbf{x}$ can be simply seen as the solution of a convex optimization problem, instead of using the optimal recovery theory as in [7]. We are looking for the vector $\mathbf{c}$ with minimum energy that obtains an interpolation $\mathbf{x}$ that is a linear function of the patches. This statement can be formulated as

$$\begin{aligned} \underset{\mathbf{x},\mathbf{c}}{\text{minimize}} \quad & \|\mathbf{c}\|^2, \\ \text{subject to} \quad & \mathbf{S}\mathbf{c} = \mathbf{x}. \end{aligned} \tag{5}$$

Without any additional constraints, the optimal solution of (5) is $\mathbf{x}^\star = \mathbf{0}$ and $\mathbf{c}^\star = \mathbf{0}$. The information coming from the signal being interpolated should be included in the formulation to obtain meaningful solutions. Previous knowledge about $\mathbf{x}$ is available since only some of its components have to be interpolated. Typically, if a decimation by two has been performed in both image directions, then one of every four elements of $\mathbf{x}$ is already known (the black pixels in Figure 1). Another possible case is the following: it may be known that the original high density signal has been averaged before a decimation. In both cases, a linear constraint on the data is known and it may be added to the formulation (5). The linear constraint is denoted by $\mathbf{A}^T\mathbf{x} = \mathbf{b}$. In the first case, the columns of matrix $\mathbf{A}$ are formed by canonical vectors $\mathbf{e}_i$, being the 1's located at the position of the known sample. The respective position of vector $\mathbf{b}$ has the value of the sample. An illustrative example for the second case is the following. Assume that the pixel value is the average of four high density neighbors, then there would be 1/4 at each of their corresponding positions in a column of $\mathbf{A}$. Whatever the linear

constraints, they are included in (5) to reach the formulation,

$$\begin{aligned} \underset{\mathbf{x},\mathbf{c}}{\text{minimize}} \quad & \|\mathbf{c}\|^2, \\ \text{subject to} \quad & \mathbf{S}\mathbf{c} = \mathbf{x}, \\ & \mathbf{A}^T\mathbf{x} = \mathbf{b}. \end{aligned} \tag{6}$$

The solution of this problem is

$$\mathbf{x}^\star = \mathbf{S}\mathbf{S}^T\mathbf{A}\left(\mathbf{A}^T\mathbf{S}\mathbf{S}^T\mathbf{A}\right)^{-1}\mathbf{b}, \tag{7}$$

which is the least square solution for the quadratic norm determined by $\mathbf{S}\mathbf{S}^T$ and the linear constraints $\mathbf{A}^T\mathbf{x} = \mathbf{b}$.

Note that the solution vectors can be seen as new data patches, better in some sense than the originally used by the algorithm. These solution vectors may be provided to a subsequent iteration of the algorithm, thus improving initial results.

Taking the expectation in (7), the formulation can be made *global*. In this case, the quadratic class is determined by the correlation matrix $\mathbf{R} = \mathbb{E}[\mathbf{S}\mathbf{S}^T]$. The equivalent global formulation of (6) is

$$\begin{aligned} \underset{\mathbf{x}}{\text{minimize}} \quad & \mathbf{x}^T\mathbf{R}^{-1}\mathbf{x}, \\ \text{subject to} \quad & \mathbf{A}^T\mathbf{x} = \mathbf{b} \end{aligned} \tag{8}$$

and the corresponding solution is

$$\mathbf{x}^\star = \mathbf{R}\mathbf{A}\left(\mathbf{A}^T\mathbf{R}\mathbf{A}\right)^{-1}\mathbf{b}. \tag{9}$$

To sum up, this formulation is useful to construct locally adapted as well as global interpolations. Global interpolation means that a quadratic model (via the autocorrelation matrix) is used for the whole image. If local data is available, the example patches are a good reference for the local quadratic interpolation.

Additional knowledge may easily be included in the formulation thanks to its flexibility. In the next section, several alternative formulations are proposed that modify the presented one in different ways.

3. ALTERNATIVE FORMULATIONS

The initial formulation (6) and its solution give a good interpolation, which is optimal in the specified sense. However, the problem statement may be further refined including additional knowledge, from the local data or from the given application. Knowledge is introduced in the formulation by modifying the objective function or by adding new constraints to the existing ones. Various alternative formulations are described in the following.

3.1. Signal bound constraint

The data from an image is expressed with a certain number of bits, let us say *nbits* bits. Then, assume without loss of generality that the value of any component of $\mathbf{x}$ is low-bounded by 0 and up-bounded by $2^{\text{nbits}} - 1$. This is an additional constraint that may be included in the problem statement as

$$\begin{aligned} \underset{\mathbf{x},\mathbf{c}}{\text{minimize}} \quad & \|\mathbf{c}\|^2, \\ \text{subject to} \quad & \mathbf{S}\mathbf{c} = \mathbf{x}, \\ & \mathbf{A}^T\mathbf{x} = \mathbf{b}, \\ & \mathbf{0} \le \mathbf{x} \le \left(2^{\text{nbits}} - 1\right) \cdot \mathbf{1}, \end{aligned} \tag{10}$$

where $\mathbf{0}$ ($\mathbf{1}$) is the column vector of the size of $\mathbf{x}$ containing all zeros (ones). The symbol $\le$ indicates elementwise inequality. Let us define the set

$$\mathcal{D} = \left\{\mathbf{x} \in \mathbb{R}^n \mid \mathbf{0} \le \mathbf{x} \le \left(2^{\text{nbits}} - 1\right) \cdot \mathbf{1}\right\}. \tag{11}$$

Notice that (10) is a quadratic problem with inequality linear constraints and so, it has no closed-form solution. Anyway, there exist efficient numerical algorithms [8] and widespread software packages (p.e., Matlab) that attain the optimal solution fast. However, if the optimal solution $\mathbf{x}^\star$ of (10) resides in the bounded domain $\mathcal{D}$, then a closed-form solution exists and is expressed by (7).

3.2. Weighted objective

Another refinement of (6) is to weight vector $\mathbf{c}$ in order to give more importance to the local signal patches that are closer to $\mathbf{x}$. Closer patches are supposed to be more alike than the further ones. The formulation is

$$\begin{aligned} \underset{\mathbf{x},\mathbf{c}}{\text{minimize}} \quad & \|\widetilde{\mathbf{W}}\mathbf{c}\|^2, \\ \text{subject to} \quad & \mathbf{S}\mathbf{c} = \mathbf{x}, \\ & \mathbf{A}^T\mathbf{x} = \mathbf{b}, \end{aligned} \tag{12}$$

where $\widetilde{\mathbf{W}}$ is a diagonal matrix with the weighting elements w_{ii} related to the distance of the corresponding patch (in the column i of $\mathbf{S}$) to the patch $\mathbf{x}$. Let us denote $\mathbf{W} = \widetilde{\mathbf{W}}^T\widetilde{\mathbf{W}}$, then the problem may be reformulated as

$$\begin{aligned} \underset{\mathbf{c}}{\text{minimize}} \quad & \mathbf{c}^T\mathbf{W}\mathbf{c}, \\ \text{subject to} \quad & \mathbf{A}^T\mathbf{S}\mathbf{c} = \mathbf{b}, \end{aligned} \tag{13}$$

which is solved using the Karush-Kuhn-Tucker (KKT) conditions [8, page 243]:

$$\text{KKT conditions: } \begin{cases} \mathbf{A}^T\mathbf{S}\mathbf{c} - \mathbf{b} = \mathbf{0}, \\ 2\mathbf{W}\mathbf{c} + \mathbf{S}^T\mathbf{A}\,\mu = \mathbf{0}, \end{cases} \tag{14}$$

which are equivalent to

$$\begin{pmatrix} \mathbf{A}^T\mathbf{S} & \mathbf{0} \\ 2\mathbf{W} & \mathbf{S}^T\mathbf{A} \end{pmatrix} \begin{pmatrix} \mathbf{c} \\ \mu \end{pmatrix} = \begin{pmatrix} \mathbf{b} \\ \mathbf{0} \end{pmatrix}. \tag{15}$$

The matrix in the last expression is invertible, so it is straightforward to compute the optimal vectors $\mathbf{c}^\star$ and $\mathbf{x}^\star$,

$$\begin{aligned} \mathbf{c}^\star &= \mathbf{W}^{-1}\mathbf{S}^T\mathbf{A}\left(\mathbf{A}^T\mathbf{S}\mathbf{W}^{-1}\mathbf{S}^T\mathbf{A}\right)^{-1}\mathbf{b}, \\ \mathbf{x}^\star &= \mathbf{S}\mathbf{W}^{-1}\mathbf{S}^T\mathbf{A}\left(\mathbf{A}^T\mathbf{S}\mathbf{W}^{-1}\mathbf{S}^T\mathbf{A}\right)^{-1}\mathbf{b}. \end{aligned} \tag{16}$$

The solution (16) corresponds to the orthogonal projection of $\mathbf{0}$ onto the subspace spanned by $\widetilde{\mathbf{W}}^{-1}\mathbf{S}^T\mathbf{A}$. The initial projection subspace $\mathbf{S}^T\mathbf{A}$ is modified according to the weight given to each of the patches.

3.3. Energy penalizing objective

A possible modification of (6) is to limit vector $\mathbf{x}$ energy by introducing a penalizing factor in the objective function. The two objectives are merged through a parameter γ that balances their importance. The formulation is

$$\begin{aligned} \underset{\mathbf{x},\mathbf{c}}{\text{minimize}} \quad & \gamma\|\widetilde{\mathbf{W}}\mathbf{c}\|^2 + (1-\gamma)\|\mathbf{x}\|^2, \\ \text{subject to} \quad & \mathbf{S}\mathbf{c} = \mathbf{x}, \\ & \mathbf{A}^T\mathbf{x} = \mathbf{b}, \end{aligned} \tag{17}$$

which is equivalent to

$$\begin{aligned} \underset{\mathbf{x},\mathbf{c}}{\text{minimize}} \quad & \begin{pmatrix}\mathbf{c}^T & \mathbf{x}^T\end{pmatrix}\begin{pmatrix}\gamma\mathbf{W} & \mathbf{0} \\ \mathbf{0} & (1-\gamma)\mathbf{I}\end{pmatrix}\begin{pmatrix}\mathbf{c} \\ \mathbf{x}\end{pmatrix}, \\ \text{subject to} \quad & \begin{pmatrix}\mathbf{0} & \mathbf{A}^T \\ \mathbf{S} & -\mathbf{I}\end{pmatrix}\begin{pmatrix}\mathbf{c} \\ \mathbf{x}\end{pmatrix} = \begin{pmatrix}\mathbf{b} \\ \mathbf{0}\end{pmatrix}. \end{aligned} \tag{18}$$

The variables to minimize are $\mathbf{c}$ and $\mathbf{x}$. All the constraints are linear with equality. KKT conditions are established. The solution is

$$\mathbf{x}^\star = \begin{cases} \mathbf{A}(\mathbf{A}^T\mathbf{A})^{-1}, & \text{if } \gamma = 0, \\ (\mathbf{I}-\mathbf{F}^{-1})\mathbf{A}(\mathbf{A}^T(\mathbf{I}-\mathbf{F}^{-1})\mathbf{A})^{-1}\mathbf{b}, & \text{if } 0 < \gamma < 1, \\ \mathbf{S}\mathbf{W}^{-1}\mathbf{S}^T\mathbf{A}(\mathbf{A}^T\mathbf{S}\mathbf{W}^{-1}\mathbf{S}^T\mathbf{A})^{-1}\mathbf{b}, & \text{if } \gamma = 1, \end{cases} \tag{19}$$

where $\mathbf{F}$ is introduced to make the expression clearer,

$$\mathbf{F} = \frac{1-\gamma}{\gamma}\mathbf{S}\mathbf{W}^{-1}\mathbf{S}^T + \mathbf{I}. \tag{20}$$

Parameter γ balances the weight of each criterion. If $\gamma = 0$, then the solution is the least squares onto the linear subspace defined by the constraints $\mathbf{A}^T\mathbf{x} = \mathbf{b}$. On the other hand, the energy of $\mathbf{x}$ has no relevance for $\gamma = 1$, and the solution reduces to (16). Intermediate solutions are obtained for $0 < \gamma < 1$.

3.4. Signal regularizing objective

An interesting refinement is to include a regularization factor as part of the objective function. Let us define the differential matrix $\mathbf{D}$, which computes the differences between elements of $\mathbf{x}$. Typically, rows of $\mathbf{D}$ are all zeros except a 1 and a -1 corresponding to positions of neighboring data, that is, neighboring samples in a 1-D signal or neighboring pixels in an image. The new problem statement is

$$\begin{aligned} \underset{\mathbf{x},\mathbf{c}}{\text{minimize}} \quad & \|\widetilde{\mathbf{W}}\mathbf{c}\|^2 + \delta\|\mathbf{D}\mathbf{x}\|^2, \\ \text{subject to} \quad & \mathbf{S}\mathbf{c} = \mathbf{x}, \\ & \mathbf{A}^T\mathbf{x} = \mathbf{b}. \end{aligned} \tag{21}$$

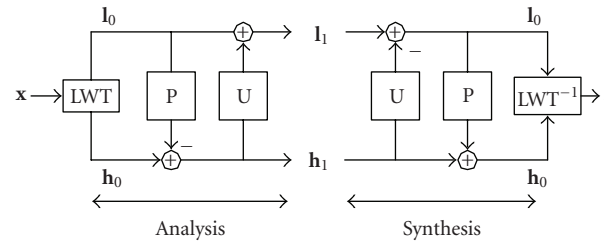

Figure 2: Classical lifting scheme.

The problem has a unique solution if $\mathbf{W}$ and $\mathbf{D}^T\mathbf{D}$ are invertible matrices. $\mathbf{W}$ is a weight matrix chosen to be full rank. However, $\mathbf{D}^T\mathbf{D}$ is singular as defined because any constant vector belongs to the kernel of the matrix (since it is the product of two differential matrices). It may be made full rank by diagonal loading or by adding a constant row to $\mathbf{D}$. The latter option has the advantage to introduce the energy weighting factor of (17) in the formulation. More or less weight is given to the energy criterion depending on the value of the constant row. Whatever the choice, the optimal solution is

$$\mathbf{x}^\star = \mathbf{M}(\mathbf{I}-\mathbf{F}^{-1}\mathbf{M})\mathbf{A}(\mathbf{A}^T\mathbf{M}(\mathbf{I}-\mathbf{F}^{-1}\mathbf{M})\mathbf{A})^{-1}\mathbf{b}, \tag{22}$$

where $\mathbf{M} = (\mathbf{D}^T\mathbf{D})^{-1}$. In general, $\mathbf{F}$ is an invertible matrix and it is defined as

$$\mathbf{F} = \delta\mathbf{S}\mathbf{W}^{-1}\mathbf{S}^T + \mathbf{M}. \tag{23}$$

In the following sections, the lifting scheme is reviewed and the connection between interpolation and lifting step design is established. It is illustrated that *good* interpolations lead to *good* lifting steps.

4. LIFTING SCHEME

The linear lifting scheme (Figure 2) comprises the following parts.

(a) Lazy wavelet transform (LWT) of the input data $\mathbf{x}$ into two subsignals.
   (i) An approximation or lowpass signal $\mathbf{l}_0$ formed by the even samples of $\mathbf{x}$.
   (ii) A detail or highpass signal $\mathbf{h}_0$ formed by the odd samples of $\mathbf{x}$.

(b) Prediction lifting step (PLS) and update lifting step (ULS), for $i = 1, \ldots, L$.
   (i) Prediction $\mathbf{p}_i$ of the detail signal with the $\mathbf{l}_{i-1}$ samples:

$$h_i[n] = h_{i-1}[n] - \mathbf{p}_i^T\mathbf{l}_{i-1}[n]. \tag{24}$$

(ii) Update $\mathbf{u}_i$ of the approximation signal with the $\mathbf{h}_i$ samples:

$$l_i[n] = l_{i-1}[n] + \mathbf{u}_i^T \mathbf{h}_i[n]. \tag{25}$$

(c) Output data: the transform coefficients $\mathbf{l}_L$ and $\mathbf{h}_L$.

Lifting steps improve the initial lazy wavelet transform properties. Possibly, input data may be any other wavelet transform with some properties we want to improve. Several prediction and update steps ($L > 1$) may be concatenated in order to reach the desired properties for the wavelet basis.

A multiresolution decomposition of $\mathbf{x}$,

$$\begin{aligned}\mathbf{x} \longrightarrow (\mathbf{l}, \mathbf{h}) = \left(\mathbf{l}^{(1)}, \mathbf{h}^{(1)}\right) \longrightarrow \left(\mathbf{l}^{(2)}, \mathbf{h}^{(2)}, \mathbf{h}\right) \longrightarrow \cdots \\ \longrightarrow \left(\mathbf{l}^{(K)}, \mathbf{h}^{(K)}, \mathbf{h}^{(K-1)}, \ldots, \mathbf{h}\right),\end{aligned} \tag{26}$$

is attained by plugging the approximated signal $\mathbf{l}_L$ into another lifting step block, obtaining $\mathbf{l}^{(2)}$ and $\mathbf{h}^{(2)}$. The process is iterated on $\mathbf{l}^{(k)}$.

The JPEG2000 standard [9] computes the discrete wavelet transform via the lifting scheme. The 5/3 wavelet is employed for lossy-to-lossless compression, so it is a good reference for comparison purposes. The 5/3 wavelet PLS is $\mathbf{p}_1 = (1/2 \;\; 1/2)^T$ and the ULS is $\mathbf{u}_1 = (1/4 \;\; 1/4)^T$.

A relevant point in the linear setting is that a wavelet transform coefficient is the inner product of a wavelet or scaling basis vector $\mathbf{w}_i$ with the input signal. Using this notation, coefficients $h[n]$ and $l[n]$ arise from $h[n] = \mathbf{w}_{h[n]}^T \mathbf{x}$ and $l[n] = \mathbf{w}_{l[n]}^T \mathbf{x}$, respectively. For instance, the 5/3 lowpass or scaling basis vectors have the form

$$\mathbf{w}_{l_1[n]} = \left(\cdots \;\; 0 \;\; \frac{-1}{8} \;\; \frac{2}{8} \;\; \frac{6}{8} \;\; \frac{2}{8} \;\; \frac{-1}{8} \;\; 0 \;\; \cdots\right)^T, \tag{27}$$

being equal to the $\mathbf{0}$ vector except for the locations from $2n-2$ to $2n+2$. Meanwhile, the highpass or wavelet basis vectors have the form

$$\mathbf{w}_{h_1[n]} = \left(\cdots \;\; 0 \;\; 0 \;\; \frac{-1}{2} \;\; 1 \;\; \frac{-1}{2} \;\; 0 \;\; 0 \;\; \cdots\right)^T, \tag{28}$$

being the $\mathbf{0}$ vector except for the positions $2n$, $2n+1$, and $2n+2$. Note that the position indices take into account the downsampling, which in the lifting scheme is performed at the LWT stage.

If no quantization is applied, the resulting wavelet coefficients arising from the lifting and from the inner product are the same. This identity is used in the next sections to connect quadratic interpolation with linear constraints and lifting design.

5. PREDICTION STEP DESIGN

The interpolation formulations presented in Sections 2 and 3 may be used for the construction of local adapted as well as global interpolative predictions. Remarkably, the same formulation introducing the linear equality constraints due to the inner product of the wavelet transform permits the construction of second PLS (noted $\mathbf{p}_2$).

A second PLS $\mathbf{p}_2$ predicts a coefficient $h_1[n]$ using a set of neighboring approximate samples, which are denoted by $\mathbf{l}_1[n]$. The PLS $\mathbf{p}_2$ aims at obtaining a predicted value $h_2[n]$,

$$h_2[n] = h_1[n] - \widehat{h}_1[n] = h_1[n] - \mathbf{p}_2^T \mathbf{l}_1[n], \tag{29}$$

that improves the initial detail samples properties in order to compress them efficiently. An important observation is that the coefficients $\mathbf{l}_1[n]$ constitute a low-resolution signal version that may be interpolated using any of the derivations introduced in previous sections. An optimal interpolation $\mathbf{x}^\star$ (which is an estimation of $\mathbf{x}$) is used to estimate $h_1[n]$ through the inner product with the known wavelet basis vector $\mathbf{w}_{h_1[n]}$. Thus, the estimated coefficient is

$$\widehat{h}_1[n] = \mathbf{w}_{h_1[n]}^T \mathbf{x}^\star. \tag{30}$$

The approximate coefficients linear constraints are included in any of the quadratic interpolation formulations (p.e., in expression (6)). Matrix $\mathbf{A}$ columns are now formed by vectors $\mathbf{w}_{l_1[n]}$, which are the basis vectors of each neighbor $l_1[n]$ in $\mathbf{l}_1[n]$ employed for the PLS. The independent term is $\mathbf{b} = \mathbf{l}_1[n]$. If the predicted value $\widehat{h}_1[n]$ is found by using the optimal interpolation vector in (9), then

$$\widehat{h}_1[n] = \mathbf{w}_{h_1[n]}^T \mathbf{x}^\star = \mathbf{w}_{h_1[n]}^T \mathbf{R}\mathbf{A}\left(\mathbf{A}^T\mathbf{R}\mathbf{A}\right)^{-1}\mathbf{b} = \mathbf{p}_2^T \mathbf{b}, \tag{31}$$

from which the optimal PLS filter is

$$\mathbf{p}_2^\star = \left(\mathbf{A}^T\mathbf{R}\mathbf{A}\right)^{-1}\mathbf{A}^T\mathbf{R}\mathbf{w}_{h_1[n]}. \tag{32}$$

Interestingly, this filter (32) is equivalent to the one in [10] that minimizes the MSE of the second PLS, that is,

$$\mathbf{p}_2^\star = \arg\min_{\mathbf{p}_2} f_0(\mathbf{p}_2) = \mathbb{E}\left[\left(h_1[n] - \widehat{h}_1[n]\right)^2\right]. \tag{33}$$

The key point is that the optimal PLS filter $\mathbf{p}_2^\star$ arises from the optimal interpolation $\mathbf{x}^\star$. If $\mathbf{x}^\star$ is very close to the image being interpolated, then $\widehat{h}_1[n] \approx h_1[n]$ and thus, the resulting prediction works well for the coding purposes, since it reduces the $\mathbf{h}_2$ detail signal energy. This is the reason that impels to improve the interpolation methods. If one of the alternative interpolation methods works well for a given image, then the chosen second PLS should be the one arising from the use of this interpolation with the proper linear constraints.

6. UPDATE STEP DESIGN

The approach offers considerable design flexibility. The same type of construction employed for the prediction is applied to the ULS. It has been proved that the solution (7) leads to the solution of the problem (33). This last expression is properly modified to derive useful ULS. Three designs are proposed. The objective functions consider the l^2-norm of the gradient (in Sections 6.1 and 6.2) and the detail signal energy (in Section 6.3) in order to obtain linear ULS applicable to a set of images sharing similar statistics.

6.1. First ULS design

A coefficient $l_i[n]$ is updated with $\widetilde{l}_i[n] = \mathbf{u}_i^T \mathbf{h}_i[n]$. If $i = 1$, we have $l_1[n] = l_0[n] + \mathbf{u}_1^T \mathbf{h}_1[n]$. The interpolation methods may employ $\mathbf{h}_1[n]$ to obtain an estimation of $l_0[n]$ by means of the product $\mathbf{w}_{l_0[n]}^T \mathbf{x}^\star$. If the interpolation is accurate, then $l_0[n] - \mathbf{w}_{l_0[n]}^T \mathbf{x}^\star \approx 0$. Therefore, an adequate value may be added to the substraction. An interesting choice is the addition of the mean value of the approximation signal neighbors. As a result, the output signal will be smooth, which is interesting for compression purposes because smooth signal is easier to predict in the subsequent resolution levels.

Let $\mathcal{I}$ be the set of the neighboring scaling coefficients and $|\mathcal{I}|$ the cardinal of the set $\mathcal{I}$. The problem is that in the lifting structure we have no access to the value of the neighbors in $\mathcal{I}$ and their mean. Instead, we may estimate the mean through the inner product $\overline{\mathbf{w}}_{\mathcal{I}}^T \mathbf{x}^\star$, where the optimal interpolation is again employed and $\overline{\mathbf{w}}_{\mathcal{I}}$ is the mean of the neighboring approximate signal basis vectors employed to update, that is,

$$\overline{\mathbf{w}}_{\mathcal{I}} = \frac{1}{|\mathcal{I}|} \sum_{i \in \mathcal{I}} \mathbf{w}_{l[i]}. \tag{34}$$

Putting all together, the updated value is obtained,

$$l_1[n] = l_0[n] + \left(\overline{\mathbf{w}}_{\mathcal{I}} - \mathbf{w}_{l_0[n]}\right)^T \mathbf{x}^\star. \tag{35}$$

The update filter expression depends on the chosen interpolation method. If the optimal interpolation is (9), then the resulting ULS is obtained including (9) in (35),

$$\mathbf{u}^\star = \left(\mathbf{A}^T \mathbf{R} \mathbf{A}\right)^{-1} \mathbf{A}^T \mathbf{R} \left(\overline{\mathbf{w}}_{\mathcal{I}} - \mathbf{w}_{l[n]}\right). \tag{36}$$

It can be shown that the update (36) is the optimal in the sense that it minimizes the l^2-norm of the substraction between the updated coefficient $l[n] + \widetilde{l}[n]$ and the set $\mathcal{I}$ of the neighboring scaling coefficients, that is,

$$\mathbf{u}^\star = \arg\min_{\mathbf{u}} \mathbb{E}\left[\sum_{i \in \mathcal{I}} \left(l[i] - \left(l[n] + \mathbf{u}^T \mathbf{h}[n] \right)^2 \right) \right]. \tag{37}$$

The next two sections propose related lifting constructions that have an objective function similar to (37) as the point of departure.

6.2. Second ULS design

The gradient minimization is a reasonable criterion for compression purposes. However, an additional consideration on the set of approximation signal neighbors $\mathcal{I}$ may be included to the gradient-minimization objective (37).

As each sample in $\mathcal{I}$ is also updated, it is interesting to consider the minimization of the gradient of $l[n] + \widetilde{l}[n]$ with respect to the updated samples $l[i] + \widetilde{l}[i]$, for $i \in \mathcal{I}$, through still unknown update filter. To this goal, the objective function is modified in order to find the optimal update with this criterion,

$$f_0(\mathbf{u}) = \mathbb{E}\left[\sum_{i \in \mathcal{I}} \left(\left(l[i] + \widetilde{l}[i] \right) - \left(l[n] + \widetilde{l}[n] \right) \right)^2 \right], \tag{38}$$

where $\widetilde{l}[i] = \mathbf{u}^T \mathbf{h}[i]$.

The objective function is expanded taking into account that the updated coefficients bases are

$$\widetilde{\mathbf{w}}_{l[i]} = \mathbf{w}_{l[i]} + \mathbf{A}_{l[i]} \mathbf{u}, \tag{39}$$

being $\mathbf{A}_{l[i]}$ the constraint matrix relative to the position of sample $l[i]$ and $\mathbf{A} = \mathbf{A}_{l[n]}$. Then, it is differentiated with respect to $\mathbf{u}$. After that, the linear constraints $\mathbf{A}^T \mathbf{x} = \mathbf{b}$ are introduced and the definition of correlation matrix is used. Equalling the result to zero, the optimal update filter minimizing the gradient is found to be

$$\mathbf{u}^\star = \mathbf{M}^{-1} \left(\mathbf{A}^T \mathbf{R} \left(\overline{\mathbf{w}}_{\mathcal{I}} - \mathbf{w}_{l[n]} \right) + \overline{\mathbf{A}}_{\mathcal{I}}^T \mathbf{R} \mathbf{w}_{l[n]} - \overline{\mathbf{b}}_{\mathcal{I}} \right), \tag{40}$$

being

$$\mathbf{M} = \mathbf{A}^T \mathbf{R} \left(\mathbf{A} - 2\overline{\mathbf{A}}_{\mathcal{I}} \right) + \overline{\mathbf{R}}_{\mathcal{I}}, \tag{41}$$

where the mean of the different products of the bases and matrices are denoted by

$$\begin{aligned} \overline{\mathbf{A}}_{\mathcal{I}} &= \frac{1}{|\mathcal{I}|} \sum_{i \in \mathcal{I}} \mathbf{A}_{l[i]}, \\ \overline{\mathbf{R}}_{\mathcal{I}} &= \frac{1}{|\mathcal{I}|} \sum_{i \in \mathcal{I}} \mathbf{A}_{l[i]}^T \mathbf{R} \mathbf{A}_{l[i]}, \\ \overline{\mathbf{b}}_{\mathcal{I}} &= \frac{1}{|\mathcal{I}|} \sum_{i \in \mathcal{I}} \mathbf{A}_{l_0[i]}^T \mathbf{R} \mathbf{w}_{l_0[i]}. \end{aligned} \tag{42}$$

Equation (40) is very simple to compute in practice. The only differences with respect to (37) are the additional terms concerning the mean of the neighbors basis vectors, which are known. The following section modifies the objective function in another way to obtain a new ULS that is optimal in a different sense.

6.3. Third ULS design

A third type of ULS construction is proposed. The objective function is set to be the prediction error energy of the next resolution level. Thus, the prediction filter is employed to determine the basis vectors as well as the subsequent prediction error. The ULS is assumed to be the last of the decomposition. The updated samples $l_L^{(1)}[n]$ are split into even $l_L^{(1)}[2n]$ and odd $l_L^{(1)}[2n+1]$ samples that become the new approximation $l_0^{(2)}[n] = l_L^{(1)}[2n]$ and detail $h_0^{(2)}[n] = l_L^{(1)}[2n+1]$ signals, respectively. For simplicity, L is set to 1 in the following. In the next resolution level, the odd samples are predicted by the even ones and the ULS design aims to minimize the energy of this prediction. It is also assumed that the same update filter is used for even and odd samples. Therefore, the objective

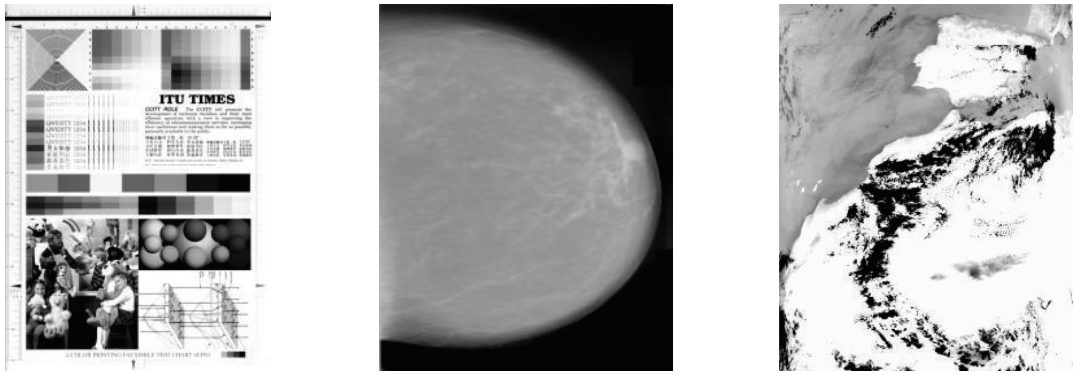

(a) (b) (c)

FIGURE 3: An image example for three image classes. (a) Synthetic image (chart), (b) mammography, and (c) remote sensing SST AfrNW 5 image.

function is

$$f_0(\mathbf{u}_1) = \mathbb{E}\Big[\left(l_1[2n+1] - \mathbf{p}_1^T \mathbf{l}_1[2n]\right)^2\Big] = \mathbb{E}\Big[\left(l_0[2n+1] + \widetilde{l}_1[2n+1] - \mathbf{p}_1^T(\mathbf{l}_0[2n] + \widetilde{\mathbf{l}}_1[2n])\right)^2\Big]. \tag{43}$$

The prediction filter length determines the number of even samples $l_1[2i]$ employed by the prediction. Employing the prediction filter taps

$$\mathbf{p}_1^T = \begin{pmatrix} \cdots & p_{1,i-1} & p_{1,i} & p_{1,i+1} & \cdots \end{pmatrix} \tag{44}$$

the objective function is set in a summation form as

$$f_0(\mathbf{u}_1) = \mathbb{E}\left[\left(\mathbf{w}_{l_0[2n+1]}^T \mathbf{x} + \mathbf{u}_1^T \mathbf{A}_{l_0[2n+1]}^T \mathbf{x} - \sum_i p_{1,i} \mathbf{w}_{l_0[2(n+i)]}^T \mathbf{x} - \sum_i p_{1,i} \mathbf{u}_1^T \mathbf{A}_{l_0[2(n+i)]}^T \mathbf{x}\right)^2\right]. \tag{45}$$

The algebraic manipulation to attain the solution is similar to the previous case. The optimal update filter is expressed as

$$\mathbf{u}_1^\star = \left(\mathbf{A}^T \mathbf{R}(\mathbf{A} - 2\overline{\mathbf{A}}_p) + \overline{\mathbf{A}}_p^T \mathbf{R} \overline{\mathbf{A}}_p\right)^{-1} (\mathbf{A} - \overline{\mathbf{A}}_p)^T \times \mathbf{R}\left(\overline{\mathbf{w}}_p - \mathbf{w}_{l_0[2n+1]}\right), \tag{46}$$

being the notation

$$\mathbf{A} = \mathbf{A}_{l_0[2n+1]}, \quad \overline{\mathbf{w}}_p = \sum_i p_{1,i} \mathbf{w}_{l_0[2(n+i)]}, \quad \overline{\mathbf{A}}_p = \sum_i p_{1,i} \mathbf{A}_{l_0[2(n+i)]}. \tag{47}$$

The final expression (46) is similar to the filter (40) obtained in the previous design. However, the optimal filter emerging from this design differs from the previous one even in the simple case that has two taps and the prediction is $\mathbf{p}_1 = (1/2 \quad 1/2)^T$. For larger supports, the difference is more remarkable. These facts are analyzed in the experiments section.

7. EXPERIMENTS AND RESULTS

7.1. Interpolation methods results

The first part of this section is devoted to a more qualitative assessment of the proposed interpolation methods. A practical reason impels to a nonexhaustive experimental setting. The proposed quadratic interpolation formulation is very rich and offers many different variants. The number of experiments to test all the possible variants is huge. The following points show such a variability and explain the basic setting for the qualitative assessment. Experiments are done for several image classes: natural, textured images, synthetic, biomedical (mammography), and remote sensing (sea surface temperature, SST) images. Figure 3 shows an example image from our database for the synthetic, mammography, and SST image classes.

(1) As stated, the formulation accepts local and global settings. *Global* means that the same quadratic class is selected for the whole image. In this case, the image model should be chosen. For the local adaptive interpolation, the local patches size and support have to be selected. In the experiments below, the choice is 4×4 and 8×8, respectively. Furthermore, an initial interpolation is required. Different choices exist to this goal, the bicubic interpolation being the preferred one. Finally, the patches may be extracted from other similar images or images from the same class.

(2) The interpolation method output may be re-introduced in the algorithm as an initial interpolation. The number of iterations may affect the final result and it should be determined. The experiments below do not iterate if nothing

else is stated. Usually, one or two iterations improve the initial results, but in the subsequent iterations, the performance tends to decrease.

(3) Five interpolation methods are highlighted in the previous sections, each of which may differently behave on each image class.

(4) In addition, some of the methods are parameter-dependant. The signal regularized and the energy penalizing approaches balance two different objective functions according to a parameter (defined as γ and δ, resp.,) that has to be tuned. The weighting objective matrix $\mathbf{W}$ in (16) should be defined by the application or the image at hand. The distance weighting depends on the image type, for example, a textured image with a repeated pattern requires different weights than a highly nonstationary image.

Clearly, the casuistry is important, but a general trend may be drawn. The interpolation given by (7) has a better global behavior than the others; it outperforms the other methods and it reduces the 5/3 wavelet detail signal energy from 5% to 20% for natural, synthetic, and SST images. The results are poorer for the mammography and the texture images.

The weighted objective interpolation (16) attains very similar results to (7), being better in some cases. For instance, the interpolation error energy is around 3% smaller for the texture image set.

The signal bound constraint (10) may be useful for images with a considerable amount of high-frequency content, as the synthetic and SST classes. Some interpolation coefficients outside the bounds appear for this kind of images, and thus, the method rectifies them. However, there is no error energy reduction and certainly a computational cost increases with respect to (7).

The signal regularized solution (22) performs very well with small values of δ that give a lower weight to the regularizing factor with respect to the $\mathbf{c}$ vector l^2-norm objective. Interestingly, in the 1D case and with a difference matrix $\mathbf{D}$ relating all the neighboring samples, the objective factor $\|\mathbf{Dx}\|^2$ coincides with $\mathbf{x}^T\mathbf{R}^{-1}\mathbf{x}$ $\mathbf{R}$ being the autocorrelation matrix of a first-order autoregressive process with the autoregressive parameter $\rho \to 1$. Therefore, the signal regularized method may be seen as an interpolation mixing local signal knowledge with an image model.

Finally, it seems that the inclusion of the energy penalizing factor in the formulation is not useful for the image sets because it damages the final result. The interest resides in its relation with the signal regularized solution and for low values of γ. Maybe, this factor could be considered for highly varying images in order to avoid the apparition of extreme values.

The interpolation methods are further assessed with the ensuing experiment. The bicubic interpolation is the benchmark and the comparison criterion is the PSNR, defined as

$$\mathrm{PSNR} = 10\log_{10}\left(\frac{255^2}{\mathrm{MSE}}\right). \tag{48}$$

Table 1 shows some results concerning images with 512×512 pixels. Images are downsampled by a factor of 2. Each pixel is the average of four highdensity pixels before the downsampling. Then, images are interpolated using different methods and number of iterations. The setting resembles the inner product used in the lifting application. It may be observed in the table that the performance in terms of PSNR is better than the bicubic interpolation up to 2 dB. In addition of the PSNR performance, it was shown in [7] that the resulting signals from the solution (7) are less blurry and sharper around the existing edges. The related global interpolation solution (9) is employed in the next section to test the ULS performance.

7.2. Lifting steps: optimality considerations

The formulation derived for the lifting filters may be employed as a tool to analyze existing filters optimality. The provided basis example is the 5/3 wavelet, but the same approach is possible for any wavelet filter factorized into lifting steps.

An estimation or a model of the autocorrelation matrix $\mathbf{R}$ is required in the global optimization approaches. In the following experiments, images are assumed to be an autoregressive process of first-order (AR-1) or second-order (AR-2). The autocorrelation matrix depends on the autoregressive parameters. In the AR-1 case, $\mathbf{R}$ is completely determined by parameter ρ, while in the AR-2 case, $\mathbf{R}$ is determined by the second-order parameters a_1 and a_2.

The optimality of the 5/3 update is studied according to the AR image model. For fair comparison, the proposed ULS employ two neighbors as the 5/3 ULS. Therefore, in practice the application simply reduces to propose a coefficient different from 1/4 for the update filter (since it is symmetric). The proposals attain noticeable improvements even in this simple case.

Assuming an AR-1 process, the three linear ULS lead to optimal filter coefficients depending on ρ as depicted in Figure 4. The second and the third designs lead to similar coefficients. Meanwhile, the ULS coefficient arising from the first design is smaller for all the intervals. Asymptotically ($\rho \to 1$), the second ULS design output doubles the coefficients of first and third ones. The update filter coefficients are considerably below the 1/4 reference for the three designs and the usual ρ found in practice (which tends to be near 1). This fact agrees with the common observation that in some cases the ULS omission increases the compression performance and that the ULS is generally included in the decomposition process because of the multiresolution properties improvement. The issue of the ULS employment can be approached from the perspective given by the proposed linear ULS designs: the ULS is useful, but the correct choice is an update coefficient quite smaller than 1/4 (as the three ULS indicate for the usual ρ values).]

The optimal ULS for each of the three designs are also derived assuming a second-order autoregressive model. For a subset of the AR-2 parameters, the resulting optimal update coefficients coincide with 1/4, but not for other possible values. Figure 5 highlights this fact for the second ULS design. The figure relates the optimal update coefficient according to the given criterion with respect to the AR-2 parameters.

Table 1: Interpolation PSNR from the averaged and downsampled images using the bicubic, the initial quadratic interpolation (column noted by **A**), and the distance weighted objective (**B**) with **1** and **2** iterations, and the regularized signal objective (**C**) with **1** iteration.

PSNR (dB)	Bicubic	A-1 it.	A-2 it.	B-1 it.	B-2 it.	C-1 it.
Baboon	22.356	**23.810**	23.695	23.717	23.745	23.595
Barbara	24.296	25.653	25.741	25.610	25.753	**25.831**
Cheryl	32.736	34.161	**34.819**	34.091	34.759	33.620
Farm	20.539	22.265	**22.490**	22.176	22.486	21.963
Girl	31.693	33.232	**34.034**	33.147	33.936	32.762
Lena	30.606	32.107	**33.058**	32.049	32.960	31.583
Peppers	29.875	31.105	31.573	31.149	**31.648**	30.775

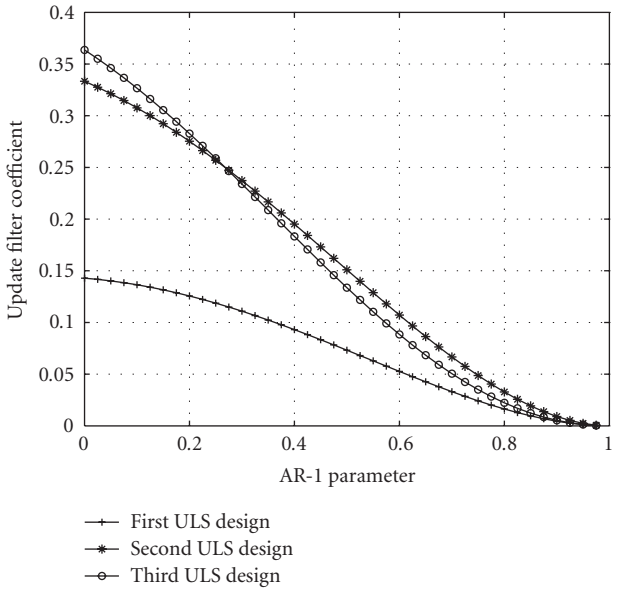

Figure 4: Update filter as function of the AR-1 parameter for the three ULS designs. The update is a two-tap symmetrical filter and so, only one coefficient is depicted. The first considered prediction is the (1/2 1/2).

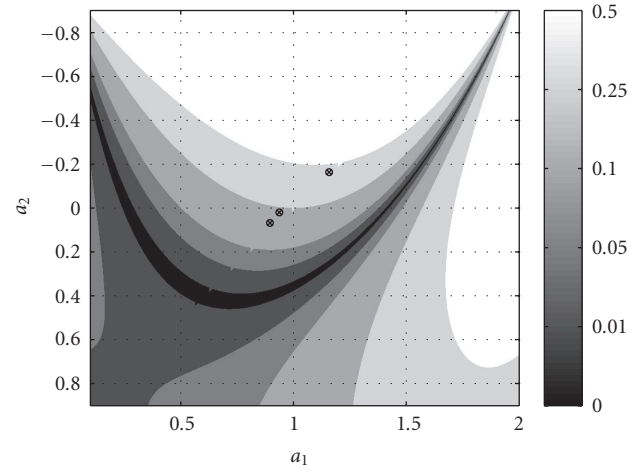

Figure 5: Six level-sets of a function of the update coefficient with respect to the AR-2 parameters. The function is the absolute value of the update coefficient minus 1/4. Thus, the resulting filter is very similar to the 5/3 in the dark areas and different in the light areas. The circles depict the mean AR-2 parameters for the synthetic, mammography, and SST image classes.

Six level sets of the update coefficient are depicted as a function of a_1 and a_2. From the figure, it is concluded that 1/4 is far from being optimal in the sense of (40) for many possible image AR-2 parameters. To position a practical reference, the three circles in Figure 5 depict the mean AR-2 parameters of the synthetic, mammography, and SST image classes.

An experiment with synthetic data is done in order to check the proposal performance for the assumed image model. An AR-1 process containing 512 samples is decomposed into three resolution levels using the 5/3 wavelet prediction followed by the 5/3 update or one of the three ULS. These four transforms are compared by computing the gradient l^2-norm of $\mathbf{l}_1^{(1)}$ and the $\mathbf{h}_1^{(2)}$ signal mean energy, which are the second and third ULS objective functions. Figure 6 shows the mean results for 1000 trials. The relative gradient and energy of the three ULS with respect to the 5/3 wavelet are depicted.

Second and third designs are almost equal and outperform 5/3 in terms of energy and gradient for all ρ except for $\rho \simeq 0.27$; value for which the three design coefficients coincide. The first design shows worse performances, in particular for the case of small ρ. However, this design has more flexibility and may incorporate additional knowledge that leads to a better image model.

7.3. Coding results

This section applies the lifting filters to image coding. The 1D filters are applied in a separable way.

7.3.1. Optimal ULS for image classes

The AR-1 parameter is estimated for three image classes. Therefore, the model is useful for a whole corpus of images instead of being local. Synthetic, mammography, and SST images are used. Each corpus contains 15 images. The correlation matrix is determined by the AR-1 parameter, and it is plugged into (36) in order to obtain an update filter

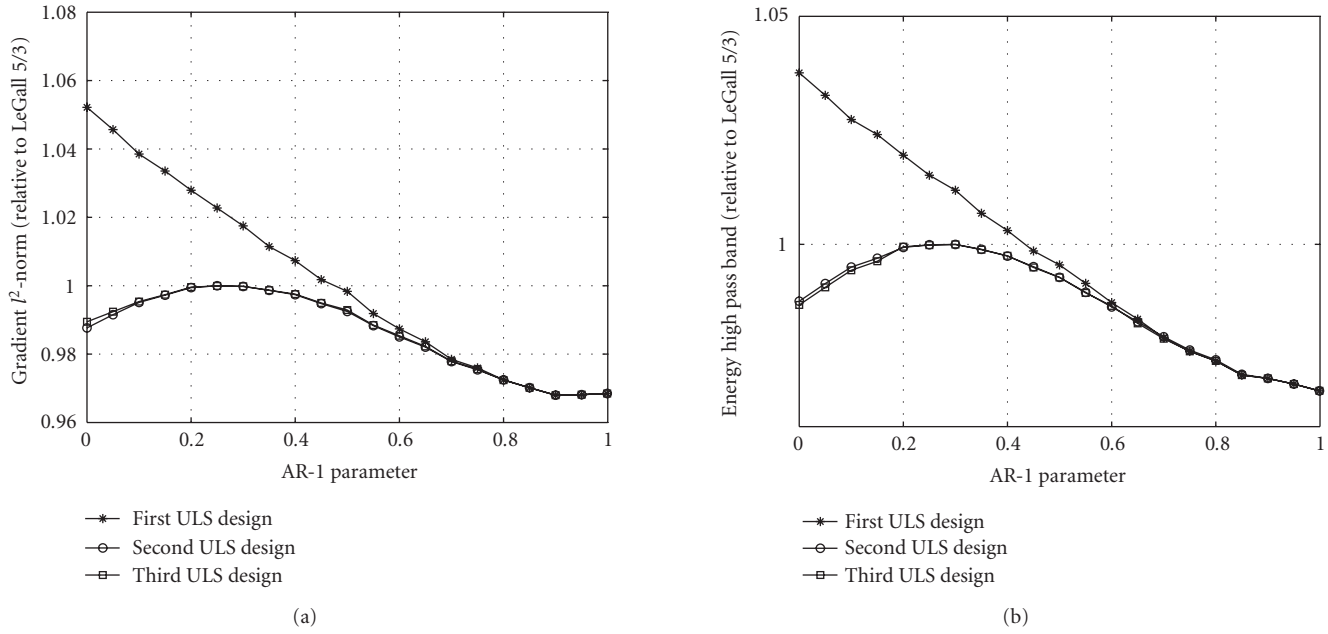

Figure 6: (a) Relative gradient of $\mathbf{l}_1$ for the optimal ULS with respect to the 5/3 wavelet, and (b) relative energy of $\mathbf{h}_1^{(2)}$ for the optimal ULS with respect to the 5/3.

Table 2: Compression results with JPEG2000 using the standard 5/3 wavelet and the proposed optimal update with the AR-1 model for the synthetic, mammography, and SST image classes. Results are in bpp.

Rate (bpp)	5/3 wavelet	AR-1 model
Synthetic	3.832	3.508
SST	3.252	3.123
Mammography	2.349	2.358

used for all the images in a class. Image compression is performed with a four-resolution level decomposition within the JPEG2000 coder environment. Numerical results appear in Table 2 compared to the 5/3 wavelet. The proposal compression results improve those of the 5/3 for the synthetic and SST image classes, but results slightly worsen for the mammography class. The latter case is analyzed in the next experiment.

7.3.2. A refinement for mammography

The optimal ULS results are worse for the mammography image class with respect to the 5/3 wavelet. The reason may be found in the structure of this kind of images. Clearly, there are two differentiated regions: a homogenous dark one containing the background and a light heterogeneous foreground. Background pixels are found at the smaller gray values, typically less than 50. Background and foreground have distinct autocorrelation and AR parameters. The mean of both AR parameters is not optimal for any of the two regions. A more accurate approach for this class should contemplate an AR model or derive an autocorrelation matrix for each of the two regions separately.

The AR-1 and AR-2 parameters are estimated for each region. The second and third ULS are derived using both models. All the approaches lead to similar update coefficients, which are close to dyadic coefficients: 1/8 for the background and 1/32 for the foreground. Therefore, the background and foreground filters are set to $\mathbf{u}_b = (1/8 \;\; 1/8)^T$ and $\mathbf{u}_f = (1/32 \;\; 1/32)^T$, respectively.

Once the coefficients are determined, images are decomposed with a space-varying ULS that depends on the next approximation coefficient value. If this coefficient is greater than the threshold T, it means that the region is foreground and the $\mathbf{u}_f$ filter is employed. Otherwise, the region is considered to be background and the optimal filter for the background $\mathbf{u}_b$ is used:

$$l_1[n] = \begin{cases} l_0[n] + \mathbf{u}_f^T \mathbf{h}_1[n], & \text{if } l_0[n+1] > T, \\ l_0[n] + \mathbf{u}_b^T \mathbf{h}_1[n], & \text{otherwise.} \end{cases} \tag{49}$$

The decoder has to take into account this coding modification in order to be synchronized with respect to the coder and to decide the filter according to the same data.

Image compression is again performed with a four-resolution level decomposition within the JPEG2000 coder environment. The selected threshold is $T = 50$. The mean results for the 15 mammographies decrease from 2.358 bpp to 2.336 bpp.

8. CONCLUSIONS

This paper develops a linear framework employed to derive new lifting steps. The starting point is a quadratic interpolation method from which several alternatives are given. The conclusion regarding the proposed methods is that their performance in terms of PSNR is around 1.5 dB better than the bicubic interpolation when the image being interpolated has been lowpass filtered before the downsampling. However, the final result depends on the appropriate choice of the interpolation method and its parameters to the image at hand.

In a natural way, the initial interpolation formulation is used for the design of lifting steps by adding an extra set of linear equality constraints in the formulation due to the inner product of the discrete wavelet transform coefficients. This permits the design of PLS minimizing the detail signal energy and the design of ULS with approximation signal gradient criteria. Indeed, the optimal interpolation obtained with any of the precedent methods may be applied to create new PLS and ULS.

The framework is also employed for an optimality analysis of the 5/3 wavelet according to the established criteria. The main conclusion is that there are image classes for which this commonly used wavelet is not optimal. The compression results within the JPEG2000 environment confirm this observation. Also in this case, a correct choice of the image model and parameters is required to obtain the best results.

Finally, the developed lifting framework seems to be very flexible. A variety of other experiments may be envisaged as a future work. Different image models could be used to derive first and second PLS, ULS, space-varying and adaptive ULS, lifting steps on quincunx grids, and so forth. Also, it would be interesting to establish the strict relation between the interpolation performance and the performance of the lifting steps derived using this interpolation.

ACKNOWLEDGMENT

This work is partially financed by TEC2004-01914 Project of the Spanish Research Program.

REFERENCES

[1] W. Sweldens, "The lifting scheme: a custom-design construction of biorthogonal wavelets," *Applied and Computational Harmonic Analysis*, vol. 3, no. 2, pp. 186–200, 1996.

[2] A. Gouze, M. Antonini, M. Barlaud, and B. Macq, "Design of signal-adapted multidimensional lifting scheme for lossy coding," *IEEE Transactions on Image Processing*, vol. 13, no. 12, pp. 1589–1603, 2004.

[3] H. Li, G. Liu, and Z. Zhang, "Optimization of integer wavelet transforms based on difference correlation structures," *IEEE Transactions on Image Processing*, vol. 14, no. 11, pp. 1831–1847, 2005.

[4] J. Hattay, A. Benazza-Benyahia, and J.-C. Pesquet, "Adaptive lifting for multicomponent image coding through quadtree partitioning," in *Proceedings of IEEE International Conference on Acoustics, Speech and Signal Processing (ICASSP '05)*, vol. 2, pp. 213–216, Philadelphia, Pa, USA, March 2005.

[5] J. Solé and P. Salembier, "A common formulation for interpolation, prediction, and update lifting design," in *Proceedings of IEEE International Conference on Acoustics, Speech and Signal Processing (ICASSP '06)*, vol. 2, pp. 13–16, Toulouse, France, May 2006.

[6] J. Solé and P. Salembier, "Adaptive quadratic interpolation methods for lifting steps construction," in *Proceedings of the 6th IEEE International Symposium on Signal Processing and Information Technology (ISSPIT '06)*, pp. 691–696, Vancouver, Canada, August 2006.

[7] D. D. Muresan and T. W. Parks, "Adaptively Quadratic (AQua) image interpolation," *IEEE Transactions on Image Processing*, vol. 13, no. 5, pp. 690–698, 2004.

[8] S. Boyd and L. Vandenberghe, *Convex Optimization*, Cambridge University Press, Cambridge, UK, 2004.

[9] "ISO/IEC 15444-1: JPEG 2000 image coding system," ISO/IEC, 2000.

[10] A. T. Deever and S. S. Hemami, "Lossless image compression with projection-based and adaptive reversible integer wavelet transforms," *IEEE Transactions on Image Processing*, vol. 12, no. 5, pp. 489–499, 2003.